

Simulation of a Multi-pass Groove Weld and Clad Plate Using Abaqus 2D Weld GUI and Comparison with Measurements

C Parmar, CM Gill, PR Hurrell, BME Pellereau

Rolls-Royce plc, PO Box 2000, Derby, DE21 7XX

Abstract: The computer simulation of multiple layering of welds is necessary to determine the distortion and residual stresses from the welding process. The welding simulation requires thermal and structural solutions, which are usually carried out in two simulations. Once solved, the thermal transient model temperature results are read into the structural model to solve for component stresses.

This paper describes the application of the Abaqus Weld Interaction (AWI) plug-in for simulating the residual stresses in ferrite-based weld specimens. The specimens were manufactured for an ongoing research programme within Rolls-Royce plc. The two test piece specimens were a Tungsten Inert Gas (TIG) welded narrow-gap ferritic plate with 239 weld bead passes and a multi-layer Metal Inert Gas (MIG) clad plate with 33 weld beads.

The Abaqus AWI Graphical User Interface (GUI) simplifies the generation of the Finite Element (FE) models, especially in regards to creating the heat transfer properties and setting up the surfaces for the welding bead sequences.

The simulation results were compared with Deep Hole Drilling (DHD), Incremental Deep Hole Drilling (IDHD) and Neutron Diffraction (ND) measurements in actual test piece specimens. The measurements showed similar results to the simulation when comparing peak stresses, however, there were some differences; these are believed to be attributed to the 2D plane strain assumption and the fact that phase transformation was not included in the simulation.

Keywords: Residual Stress, Welding, Narrow-Gap, Clad.

1. Introduction

The simulation of multiple layering of welds is necessary to determine the distortion and Weld Residual Stresses (WRSs) from the welding process. The welding simulation requires thermal and structural Finite Element (FE) models which are carried out in two simulations. The thermal transient model once solved reads in temperatures from the results file to the structural model to resolve for component stresses.

The work carried out in this paper is part of the validation study between Deep Hole Drilling (DHD), Incremental Deep Hole Drilling (IDHD) and Neutron Diffraction (ND) measurement

results to the 2D FE model simulations for determining stress components from the As-Welded (AW) and Post-Weld Heat Treatment (PWHT) states.

2. Weld Modelling

There are a number of methods used for simulating weld modelling, however, this paper will describe the method used with the Abaqus Weld Interaction (AWI) plug-in (SIMULIA, 2010) with Abaqus/CAE (SIMULIA, 2010). The modelling technique uses a thermal model, which provides thermal loads to a structural model using the 'block-dump' method. The term 'block-dump' is where the FE model simulates the weld bead deposition in a single block in the FE model.

3. Specimens and Models

3.1 Geometry and Specimen Types

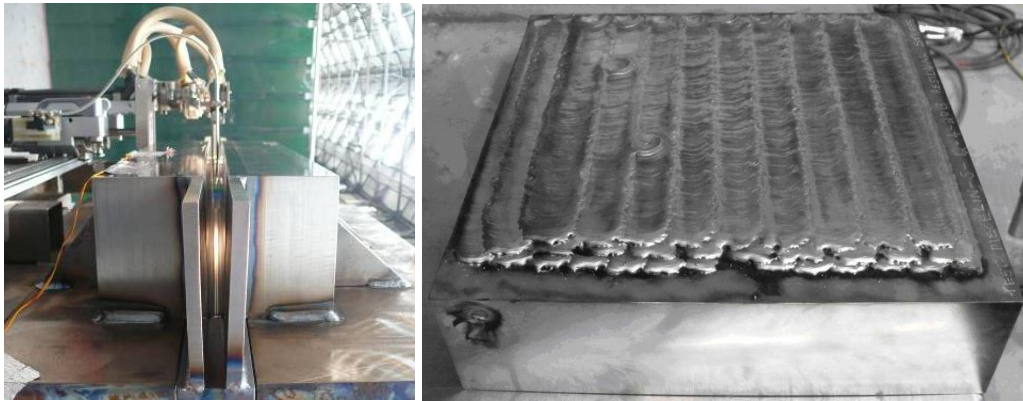
Two different weld specimens were analysed using the Abaqus AWI 2D Graphical User Interface (GUI) plug-in. The weld specimens were produced by a mechanised computer controlled welding system, which adjusted the speed, feed and energy across the specimens.

The narrow-gap Tungsten Inert Gas (TIG) specimen welded two ferritic blocks each of size 90 x 120 x 480 mm together using 239 weld beads. The welding process started with a single weld bead at the root of the cavity and finished at the top of the cavity with four weld beads. A further six weld beads were applied as a capping weld.

The flat ferritic Metal Inert Gas (MIG) clad plate of 300 x 80 x 300 mm had three layers of weld beads applied. A total of 33 weld beads were deposited in which the first layer contained 12 beads, the second 11 beads, and the third 10 beads. Two base metal plate thicknesses were investigated, 40 and 80 mm with a clad thickness of 9.5 mm.

3.2 Materials

The base material for the narrow-gap TIG weld and clad plate MIG weld specimen was SA508 Grade 4N. The base and filler material regions are illustrated in Figure 1 for the narrow-gap and clad plate specimens. The narrow-gap specimen used a 1% nickel and 0.5% molybdenum alloy ferritic filler material. The clad specimens used two filler materials on separate specimens; Alloy 82 and Type 308 L Stainless Steel (SS). The 40 mm clad plate was not simulated with Alloy 82 filler material properties. The Type 308 L filler weld was a sensitivity study on the two clad plate thicknesses (40 and 80 mm).



Narrow-Gap Specimen

Clad Plate Specimen

Figure 1. Narrow-Gap and Clad Plate Specimens.

3.3 Analysis

The FE models were rapidly constructed using the AWI plug-in in Abaqus/CAE. The pre-processing for mesh generation and material section assignments were carried out in Abaqus/CAE. The welding parameter definitions were generated in the AWI plug-in to complete the pre-processing.

The thermal model had second order DC2D8 and DC2D6 quadrilateral and triangular heat transfer elements applied, with a structured mesh in the weld regions and Heat-Affected Zone (HAZ). A free mesh was adopted in the regions of no interest. The structural model also had second order elements applied which were CPEG8R and CPEG6 (generalised plane strain elements). A total of 20,033 elements were created for the whole narrow-gap model, 11,129 elements for the 80 mm clad weld model, and 9,316 elements for the 40 mm clad weld model. The FE model meshes are illustrated in Figure 2. A mesh sensitivity study, including weld bead shapes, was used to check the adequacy of the mesh.

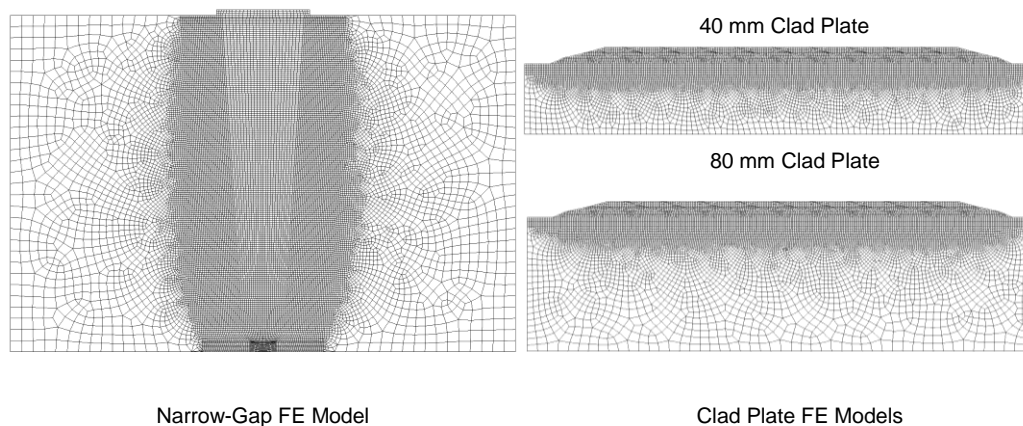


Figure 2. Finite Element Model Meshes for Simulation.

The first step for the entire model uses the ***MODEL CHANGE** flag to remove all the weld beads. Then each bead is sequentially deposited in four steps for the thermal model. The weld bead surface is then heated to the melting temperature (T_m), and where the HAZ region is identified from weld specimen slices, the HAZ sensors are placed from the fusion boundary. The four steps are:

‘Apply Torch’: During this step, a boundary condition is applied to ramp the temperature at the edges of the weld cavity where the weld bead is to be deposited up to the specified melting temperature (in this case 1,400°C). This step duration is 0.1 s.

‘Torch Hold’: During this step, the temperature boundary condition at the edges of the weld cavity is held fixed at 1,400°C and heat is allowed to soak out into the rest of the model. A FORTRAN subroutine (created automatically by the AWI plug-in) is used to set the length of this step and, therefore, control the amount of heat transferred into the model. The subroutine monitors the temperature at ‘sensor’ nodes that are located around the edge of the weld bead; when these nodes reach the target temperature of 750°C, the step is ended.

‘Torch Pause’: During this step, the elements within the weld bead that is being deposited are activated (at an initial temperature of 1,400°C) and the fixed temperature boundary condition around the edge of the bead is removed to allow heat to soak through the model. The step lasts for 1.0E-7 s.

‘Cool-down’: This step represents the model between weld passes when the heat from the most recent pass of the weld torch soaks through the component. During manufacture of the actual components an inter-pass temperature of 175°C for the narrow-gap FE model and 110°C for the clad FE models was specified. To account for this, the FORTRAN subroutine was again used to control the end of the step, with the target temperature set to 175°C or 110°C depending on the model for all the passes except for the final one, for which 21°C was applied for the narrow-gap model and 20°C for the clad model. The narrow-gap thermal model had 957 steps for 239 weld beads and the clad thermal model had 133 steps for 33 weld beads.

The last step allows the weld bead to cool down before subsequent beads are added. The structural model uses three steps in which it combines the ‘Apply Torch’ and ‘Torch Hold’ into a single step, and again, like the thermal model it removes all the weld beads in the very first step.

The thermal and structural input decks were written out by the AWI plug-in; however, modifications were made to the structural input deck, these included changing the elements to generalised plane strain, `*ELEMENT, TYPE=[CPEG8R | CPEG6]`, creating a node set of all the model nodes for PWHT, `*NSET, NSET=name`, adding a reference point for the generalised plane strain elements `*NODE`, applying idealised boundary conditions `*BOUNDARY, OP=NEW`, and changing the `*OUTPUT, FIELD, FREQUENCY=number`, flag results to reduce the size of the output database file. The structural input deck included plastic material properties, `*PLASTIC, HARDENING=KINEMATIC` with `*CREEP, LAW=TIME` and `*ANNEAL TEMPERATURE` set at T_m for both the base and weld materials. The SS weld material included further material parameters which were `*PLASTIC, HARDENING=COMBINED, DATA TYPE=PARAMETERS, NUMBER BACKSTRESSES=value` and `*CYCLIC HARDENING, PARAMETERS`.

The structural input deck was split into four separate restart runs, this was because the internal memory allocation within the Abaqus/Standard (SIMULIA, 2010) solver was limited, and subsequently, the restart flag `*RESTART, WRITE, FREQUENCY=number` from the last step of the previous input deck and `*RESTART, READ, STEP=number`, was used on the following input decks to complete the analysis simulation.

A separate input deck was created for the PWHT, which was run as a restart from the last structural weld simulation step. The PWHT was simulated at various time durations to see the effect the creep stress relaxation had in reducing the stresses from removing the high plastic strains in the weld regions using the `*VISCO, CETOL=value` flag followed by `*TEMPERATURE` in the `*STEP` level. A `*MODEL CHANGE` flag was used on all the models to remove elements that represented machining prior to PWHT. The narrow-gap model had new boundary conditions applied to simulate removing a constraint feature used during welding which is removed prior to undergoing PWHT in the furnace. The PWHT cycle is schematically illustrated in Figure 3 where all the nodes were linearly increased in temperature due to slow heating and cool-down rates.

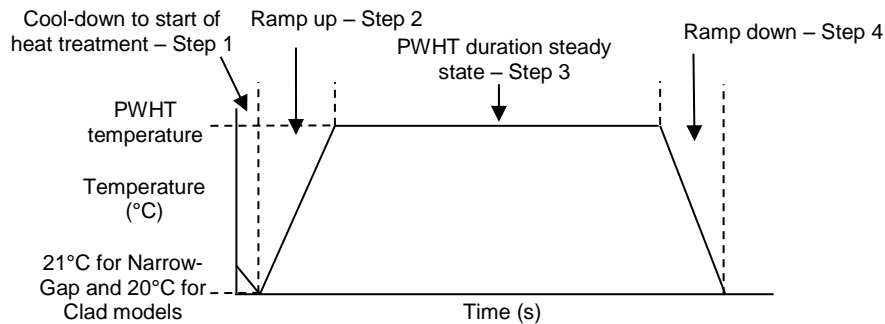


Figure 3. Post Weld Heat Treatment Cycle.

4. Results

4.1 Narrow-Gap Results

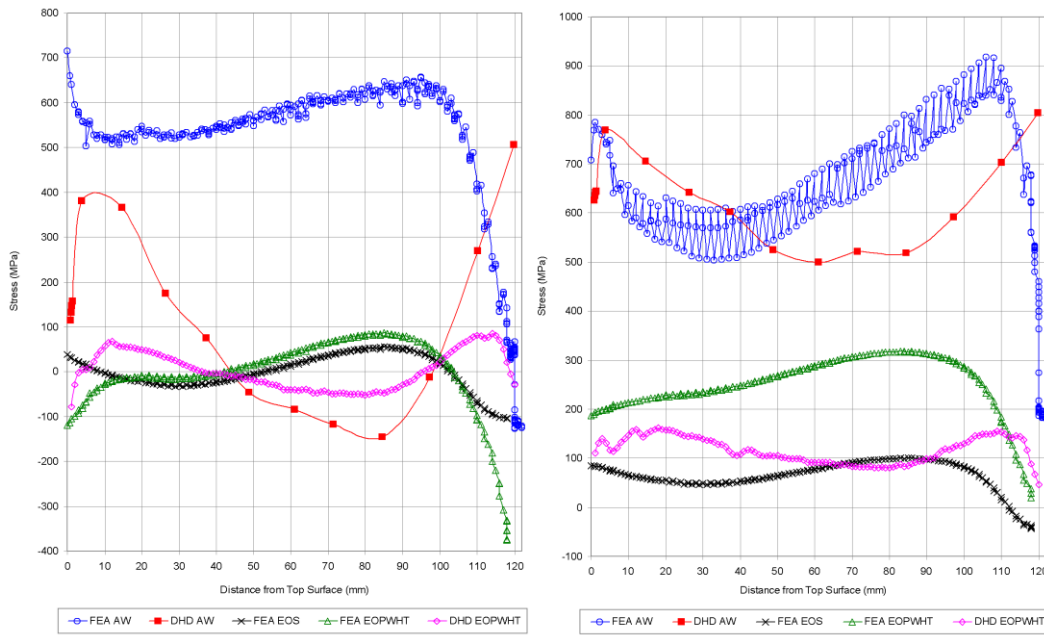
The model predicted displacement of 0.88 mm in the horizontal (lateral) direction with a 0.49 mm displacement in the through-thickness direction acting downwards. The specimen had a lateral displacement measured at 4-5 mm.

The modelled stresses were extracted at the Weld Centre Line (WCL). The Finite Element Analysis (FEA) AW transverse stress in Figure 4 illustrates a large compressive stress at the bottom weld cavity (~120 MPa) and tensile at the top (550 MPa). The compressive stress occurs due to the difference in material contraction of the weld metal to the base metal and the fact that burn-through mixture of the base and filler material was not simulated at the root ligament due to no mixed material property data being available. The weld metal possesses a larger thermal expansion coefficient and thus contracts more than the base material during the cool-down period. The FEA AW stress in the longitudinal direction, illustrated in Figure 4, is also large (735 MPa at the top cavity and 275 MPa at the root). This is expected due to the 2D plane strain assumption, which will overestimate longitudinal stresses.

The PWHT simulated for 15 hours reduced the residual stress in the transverse and longitudinal directions as shown in Figure 4 and Figure 5. The graphs show a comparison of results of FEA AW, End of Soak (EOS), and End of Post-Weld Heat Treatment (EOPWHT) compared to the DHD results for AW and EOPWHT. An increase in transverse stress is seen in the root cavity and also, a sharp change in stresses is predicted at the transition between the base and weld material for the longitudinal stresses in Figure 4. This is a modelling artefact due to the sharp transition in material properties. In reality, material mixing would occur resulting in a gradual change in material properties and stress levels. A small benefit in reducing the stresses was experienced when the PWHT soak time is extended beyond 15 hours. The maximum longitudinal stress at the WCL reduces by 40 MPa (from 340 MPa to 300 MPa) if the soak time is increased to 30 hours.

Figure 6 shows a contour plot of the maximum temperature reached at each point in the model during the analysis. Regions exceeding 1,399°C and 750°C are highlighted in the contours respectively. These regions correspond to the Fusion Zone (FZ) and HAZ and compare well with the narrow-gap specimen also shown in Figure 6, where the depth of the FZ is approximately 2 mm and the HAZ outer edge is 2-3 mm further away from the weld groove.

Figure 7 shows a contour plot of the plastic equivalent strain at the PWHT state. Most elements in the weld and parent HAZ have values in the range of 5-15% which is typical of multi-pass welds. There are some regions where the value is much higher (up to 29%). However, these are modelling artefacts due to the high stresses created at the corners of the rectangular weld beads. The typical plastic strains within the weld beads are (~20%). The PWHT initiated creep to occur, however, limited additional plasticity was experienced from the PWHT.



Transverse Stress

Longitudinal Stress

Figure 4. Narrow-Gap Transverse and Longitudinal Simulation Stress Results, Stresses are in MPa.

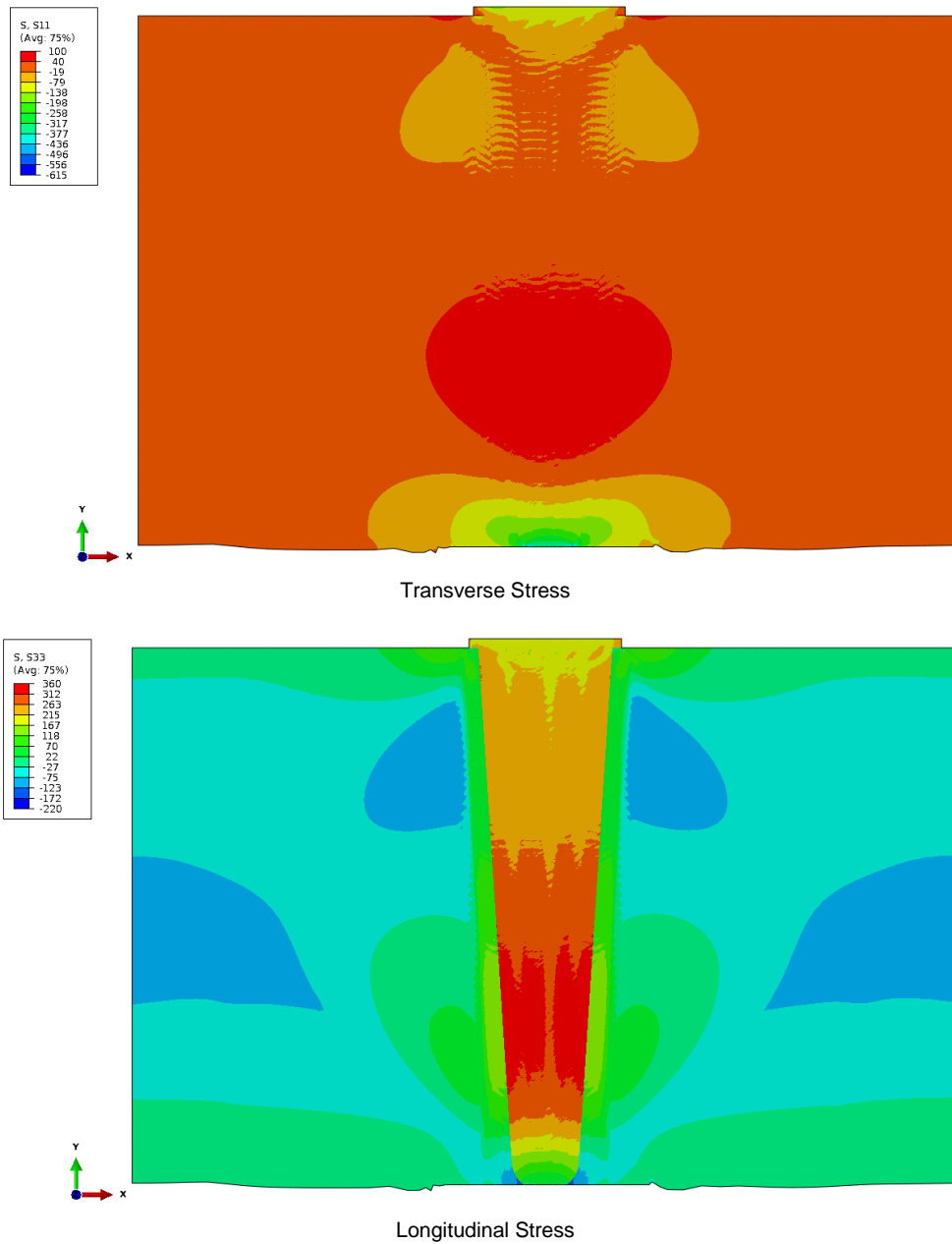


Figure 5. Narrow-Gap Transverse and Longitudinal PWHT Simulation Stress Result Contour Plots, Stresses are in MPa.

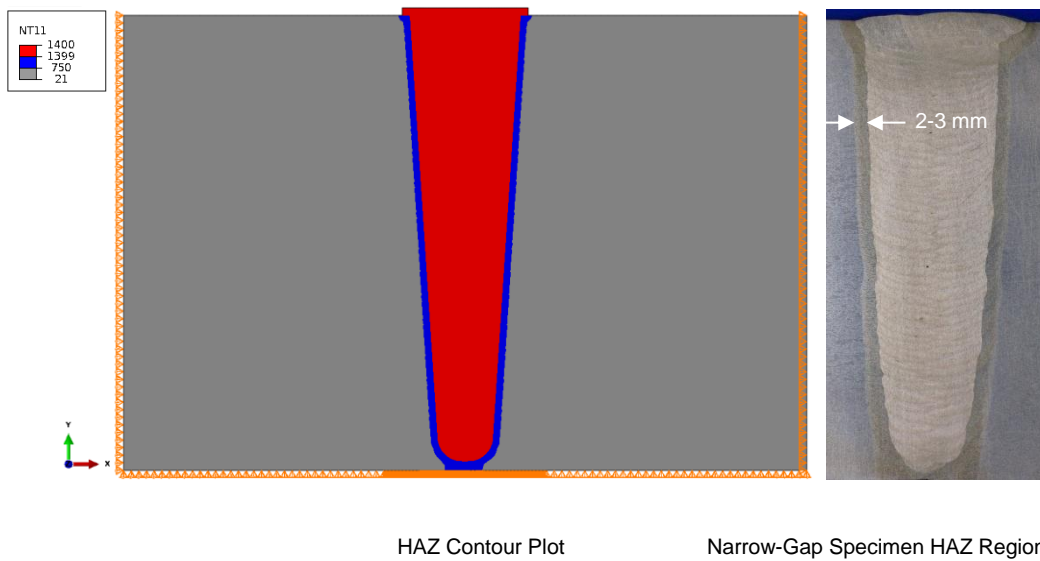


Figure 6. Narrow-Gap Simulation Results Heat Affected Zone, Temperature is in °C.

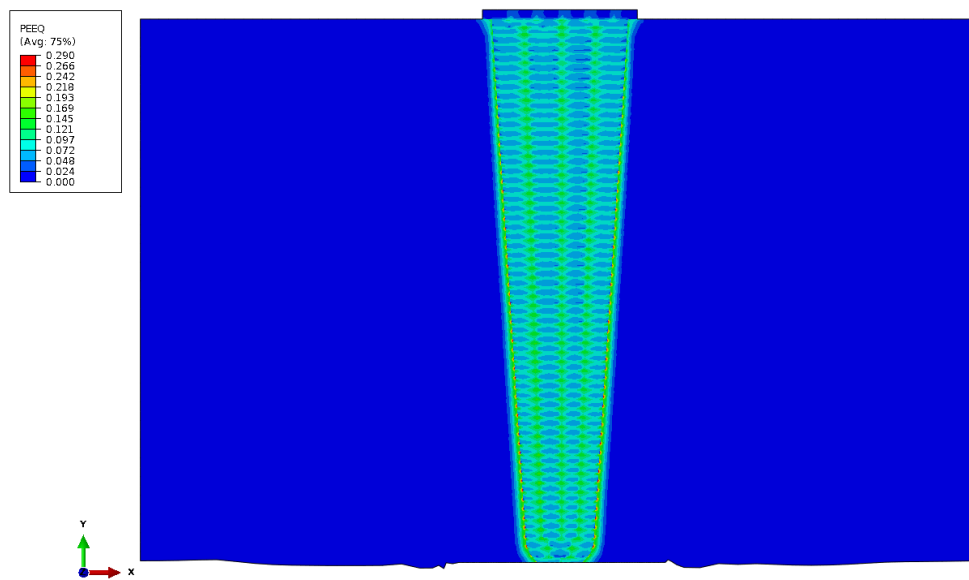


Figure 7. Narrow-Gap Plastic Equivalent Strain in PWHT State, Strain in Percent.

4.2 Clad Plate Results with Alloy 82 Weld Material

The simulation results for this model could not be compared with DHD measurements due to them not being available at the time for comparison. Therefore, only simulation results were extracted.

The model predicted displacement of 0.54 mm in the horizontal (lateral) direction with a 0.68 mm displacement in the through-thickness direction acting downwards. These displacements are due to the effect of hot cladding material contracting as it cools. These displacements applied to both the AW and PWHT states.

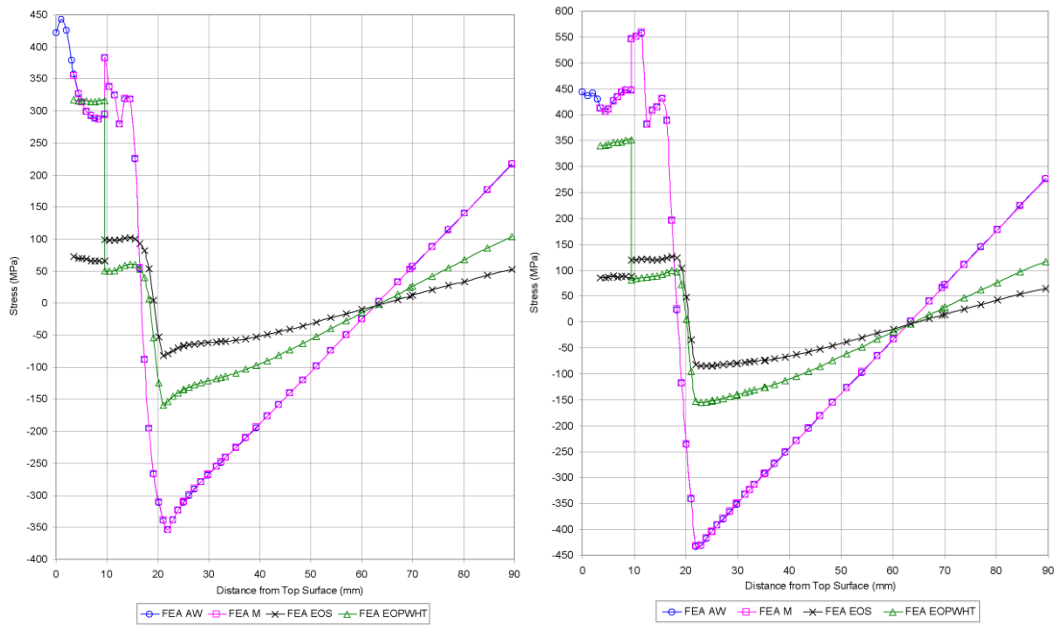
The AW transverse stress in Figure 8 shows that the back face of the plate base material stresses are tensile. Nearer to the HAZ region, the base material experiences large compressive stresses, whereas the weld metal itself has tensile stresses. The change in stresses occurs due to the difference in material contraction rates of the weld and base material. The weld material possesses a larger thermal expansion coefficient and contracts more than the base material during the cool-down period. During the simulation, the weld metal is introduced hot and contracts; the parent metal itself is 'cold' and so it resists this.

The AW longitudinal stress distribution in Figure 8 has a similar shape to the transverse stress distribution, however, the peak tensile stresses in the weld metal are higher (typically ~450 MPa compared to about ~350 MPa in the transverse direction). The result is typical of 2D WRS models, which generally overestimate the stresses in the longitudinal direction.

The PWHT was simulated for a seven-hour duration. The heat treatment reduced the residual stress in both the transverse and longitudinal directions as illustrated in Figure 8 and Figure 9. The graphs show results of the FEA simulation for AW, Machining (M) of the plate, EOS, and EOPWHT. The AW values were extracted prior to PWHT treatment where the FE model temperature was 20°C. The M values were extracted when the FE model was at 20°C, however, with the elements removed to simulate the machining process prior to PWHT. The EOS values were extracted at the EOS prior to cooling back to room temperature, and EOPWHT values were recorded from the point where the FE models temperature was ramped back to 20°C from the PWHT.

Figure 10 shows a contour plot of the maximum temperature reached at each point in the model during the analysis. Regions exceeding 1,399°C and 750°C are highlighted in the contours respectively. These regions correspond to the FZ and HAZ and compare well with the clad specimen where the depth of the FZ is approximately 2 mm and the HAZ outer edge is 2-3 mm further away from the weld.

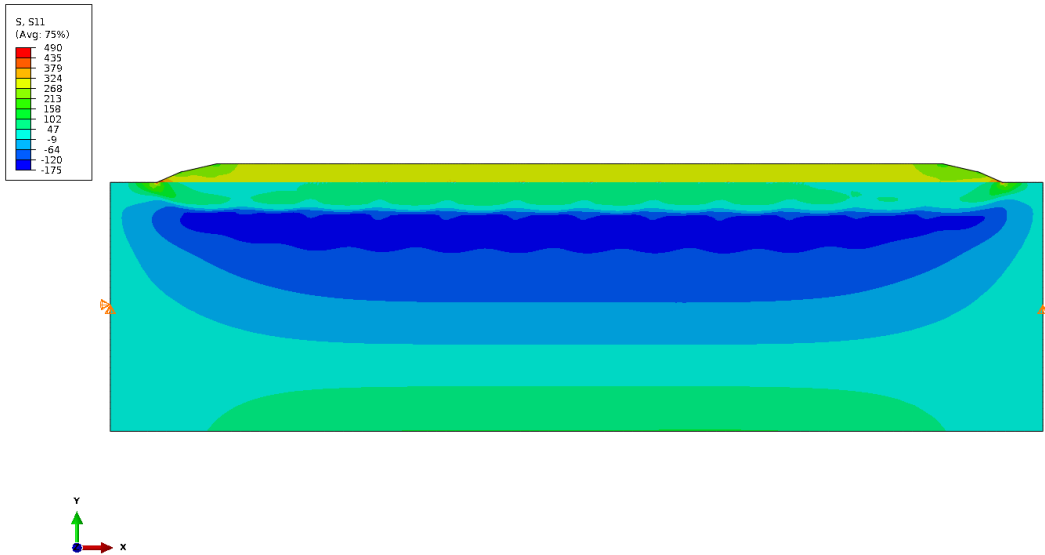
A high plastic equivalent strain of 27.7% was experienced upon the corners of the weld beads from each weld pass as illustrated in Figure 11. The resulting high plastic equivalent strain is due to the weld material cooling and then being re-heated from conduction with an adjoining weld bead during each weld bead pass and also partially a modelling artefact due the sharp corner discontinuities. This causes plastic deformation to occur during the cool-down period when the subsequent weld metal starts to cool down. The PWHT initiated creep to occur, and in doing so, no change was seen when compared to the AW conditions illustrated in Figure 11.



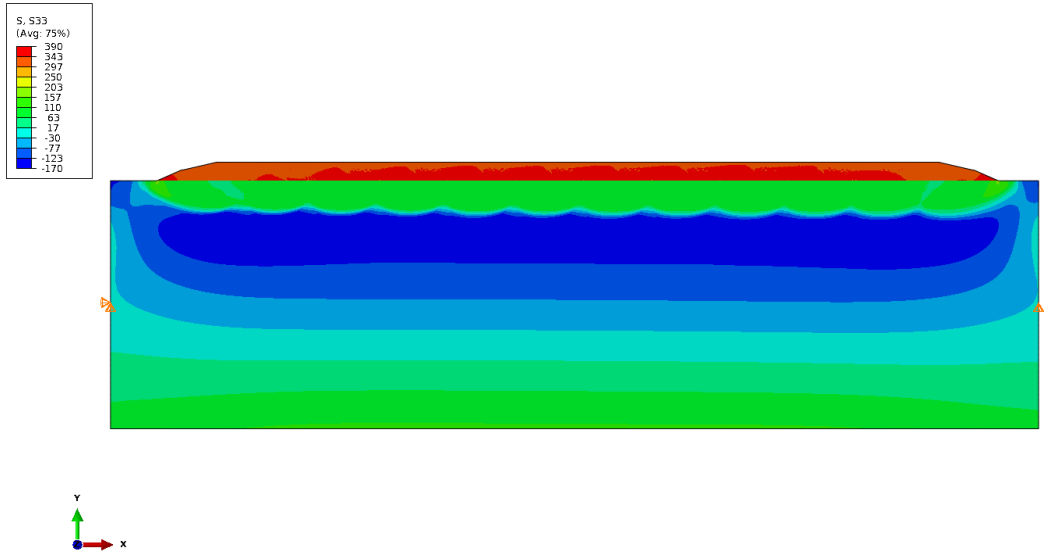
Transverse Stress

Longitudinal Stress

Figure 8. Alloy 82 Clad Plate Transverse and Longitudinal Simulation Stress Results, Stresses are in MPa.



Transverse Stress



Longitudinal Stress

Figure 9. Alloy 82 Clad Plate Transverse and Longitudinal PWHT Simulation Stress Result Contour Plots, Stresses are in MPa.

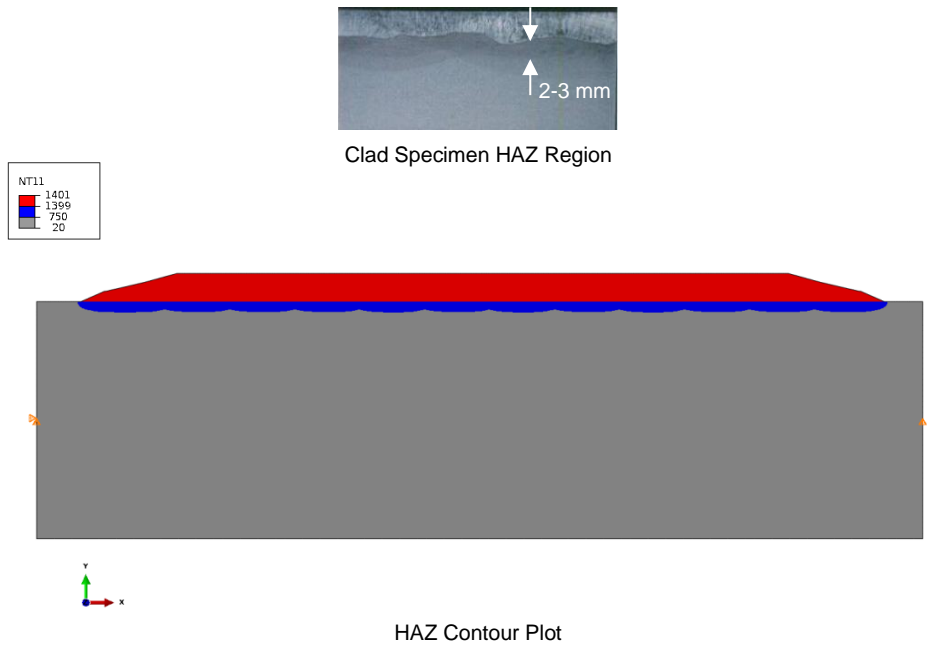


Figure 10. Alloy 82 Clad Plate Simulation Results Heat Affected Zone, Temperature is in °C.

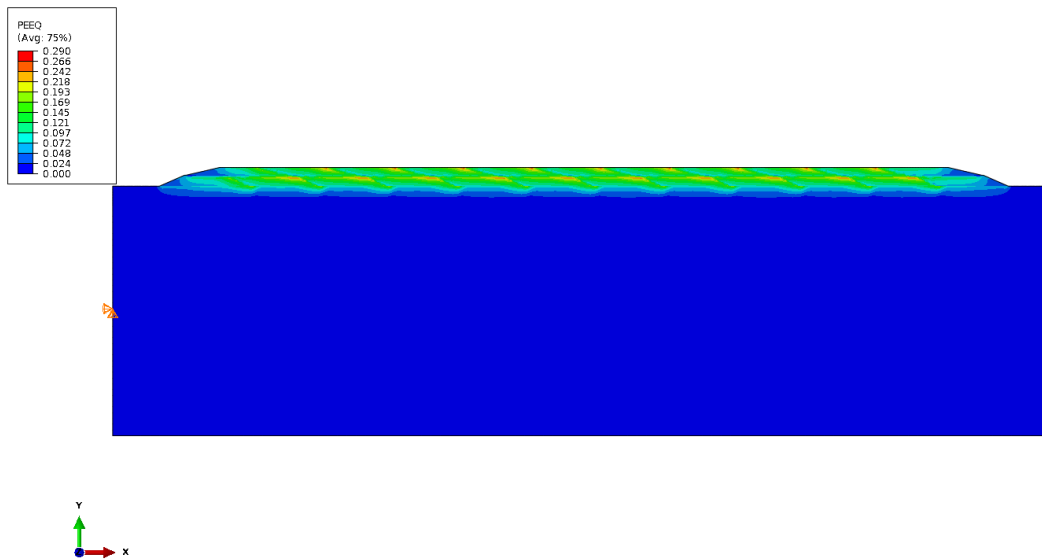


Figure 11. Alloy 82 Clad Plate Plastic Equivalent Strain in PWHT State, Strain in Percent.

4.3 Clad Plate Results with Type 308 L Stainless Steel Weld Material

The FE results presented in this section was a sensitivity study using SS weld material on two clad plate thicknesses; 40 and 80 mm. The PWHT model results showed good agreement with the stresses in the parent material immediately below the cladding. This is most likely to be due to the fact that in the simulation of the PWHT, creep is assumed only to happen during the soak when the temperature in the model is fixed at PWHT temperature. At the EOS, the WRS is reduced to less than ~120 MPa. When the model cooled down to 20°C, stresses were predicted to arise due to the differences in thermal expansion coefficient between the two materials, and since the stresses during this step are less than the material yield stress, the material behavior is entirely elastic. This effect is exacerbated by the fact that the FE model contains a step change in material properties. In reality there will be a more gradual variation due to mixing of the weld and parent metal in the FZ of the first layer of cladding material. These results are illustrated in Figure 12 and Figure 13, which are discussed in more detail in the next section.

Figure 14 shows a contour plot of the maximum temperature reached at each point in the model during the analysis for the 40 and 80 mm clad plate profiles. Regions exceeding 1,399°C and 750°C are highlighted in the contours respectively. The predicted FZ and HAZ are consistent with Rolls Royce's experience in TIG welding but cannot be confirmed as no macroscopic photograph was taken due to the specimen not being available.

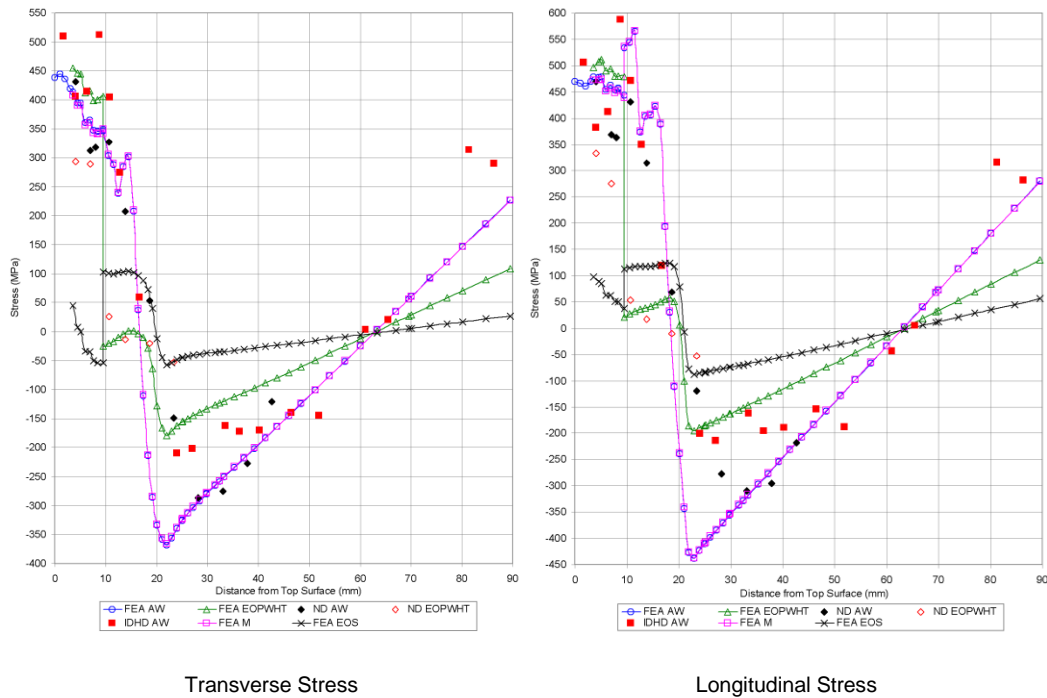


Figure 12. Type 308 L Stainless Steel 80 mm Clad Plate Transverse and Longitudinal Simulation Stress Results, Stresses are in MPa.

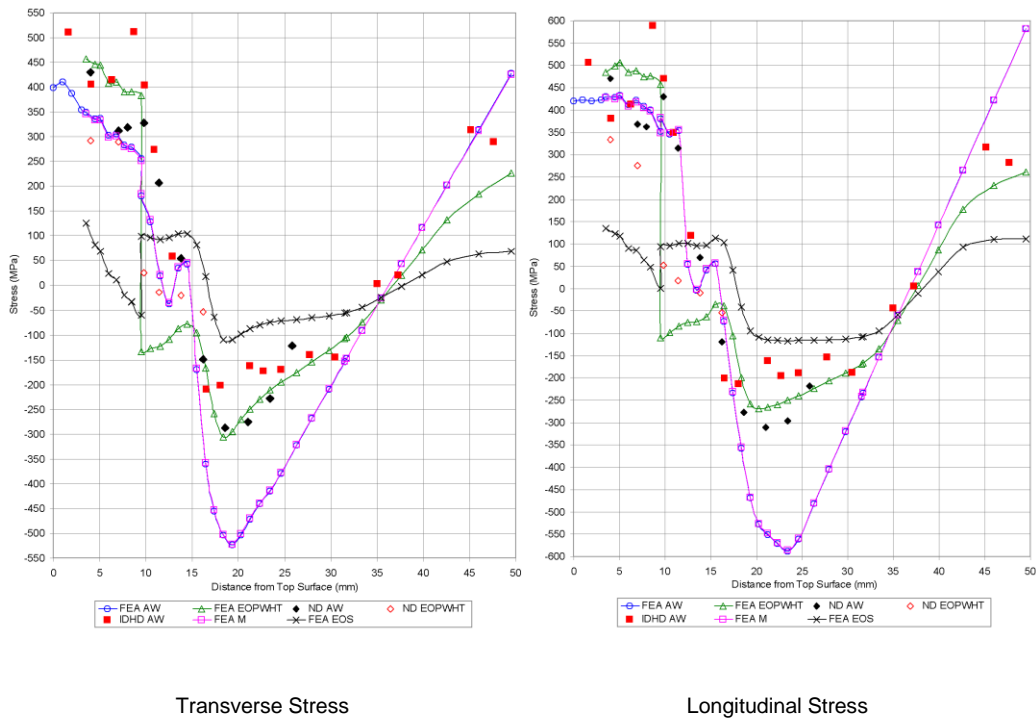
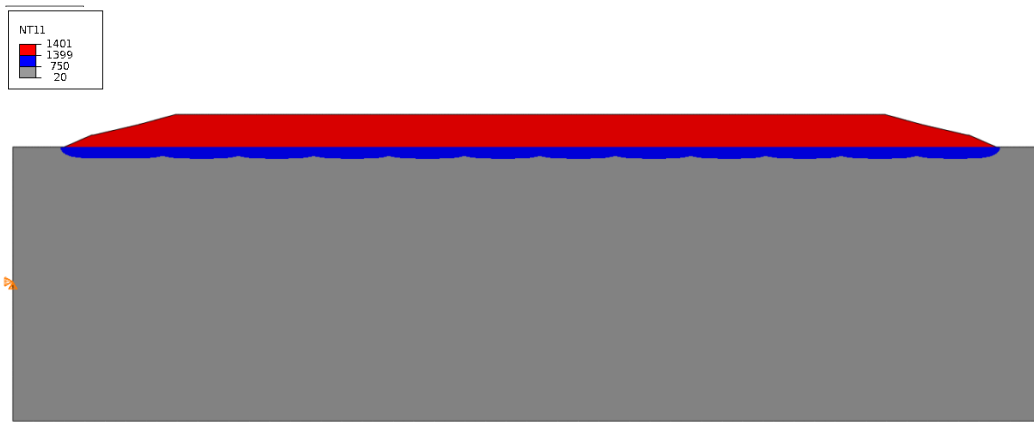
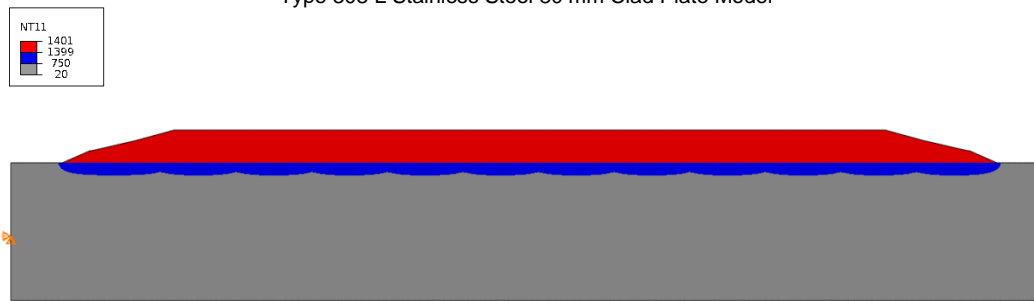


Figure 13. Type 308 L Stainless Steel 40 mm Clad Plate Transverse and Longitudinal Simulation Stress Results, Stresses are in MPa.



Type 308 L Stainless Steel 80 mm Clad Plate Model



Type 308 L Stainless Steel 40 mm Clad Plate Model

Figure 14. Type 308 L Stainless Steel Clad Plate Simulation Results Heat Affected Zone, Temperature is in °C.

5. Discussion

The narrow-gap model predicts the weld mouth closing by 0.88 mm, previous FE results in ferritic welds have shown that displacements tend to be over predicted when phase transformations are neglected. The measurements on the test specimen during manufacture show the weld mouth closing by approximately 5 mm, this suggests that in the model, the lateral constraint applied by the boundary conditions overly constrains the model, this is difficult to avoid in a simplified 2D model and will influence the predicted residual stresses.

The model representation of the weld mock-up produced transverse AW and PWHT results dissimilar to the DHD results as illustrated in Figure 4. The longitudinal stresses, however, did show slight similarity to the DHD results illustrated in Figure 4 where the FEA results were slightly more conservative. It can be also noted that the specimen contraction was in the region of 4-5 mm when compared to the FEA displacement of 0.88 mm. This has a significant effect since constraining the FE model in the lateral direction introduces high transverse stresses.

The clad model measurements for the longitudinal and transverse stresses have been made both in the AW condition and after PWHT. Figure 12 show a comparison of the 80 mm thickness FE results with the measurements; the distance values for measurements locations in the parent have been scaled from a 50 mm specimen in the through-thickness distance in order to account for the different base plate thickness (distance values of less than 9 mm have been left unchanged). The solid lines represent the FE modelling results, whereas the points are the measured data – diamonds are ND measurements and the squares are from IDHD measurements.

In the AW condition there is good agreement between the FE results and the measured values, both in the cladding (up to ~9 mm from the top surface) and in the parent material. This applied both in the longitudinal and transverse directions. After PWHT, the results do not show good agreement with the stresses in the parent material immediately below the cladding. This is most likely to be due to the fact that in the simulation of the PWHT, creep is assumed only to happen during the soak when temperature in the model is fixed at the PWHT. At the EOS, the WRS is reduced to less than 120 MPa (see EOS lines in Figure 12 and Figure 13), however, as the model cools back down to 20°C, stresses are generated due to the differences in thermal expansion coefficient between the two materials and since the stresses during this step are less than the material yield stress, the material behavior is entirely elastic. This effect is exacerbated by the fact that the FE model contains a step change in material properties (which can be seen clearly in the stress plots Figure 8, Figure 12 and Figure 13). In reality there will be a more gradual variation due to mixing of the weld and parent metal in the FZ of the first layer of cladding material.

Both cladding materials considered in this work (Alloy 82 and Type 308 L) have coefficients of thermal expansion that are higher than the value for the parent material, resulting in tensile stresses in the cladding and balancing compressive (or at least reduced tensile) stresses in the parent material. The thermal mismatch effect is much more significant for the Type 308 L cladding, as can be seen by the bigger difference between the EOS and EOPWHT predictions for the SS cladding models. In reality creep will initially continue as the component cools down and so a proportion of these thermal mismatch stresses will be relaxed during cooling, reducing the final tensile stresses in the cladding material. The cool-down rate after furnace PWHTs is slow

(typically 15°C/hour) and so the component will stay relatively hot long enough for creep to occur.

6. Conclusion

The FE model and the DHD measurements provided similar results for longitudinal stresses in the AW state, however, the FE model predicted much higher transverse stresses than the DHD measurements. This difference is considered to be due to the rigid boundary conditions in the FE model. Following PWHT, similar magnitudes of residual stress were found between the FE model and the DHD measurements for both the longitudinal and transverse weld stresses. The FE results demonstrated that the WRS is relatively insensitive to variations in length of PWHT soak from 7 hours to 30 hours.

The cladding in the AW condition predicted similar stress distributions in the longitudinal and transverse directions. The longitudinal stresses are generally slightly larger, with tensile stresses up to 450 MPa in the cladding material and up to 550 MPa in the parent FZ and HAZ. Below the HAZ there is a rapid transition into compressive stress (with peak compressive stress of -430 MPa) and a balancing tensile stress of 275 MPa on the back surface of the plate.

After PWHT, the stresses are reduced, particularly in the parent material; however, tensile stresses of up to 350 MPa are still predicted in the cladding material. This is likely to be an over prediction, however, since there are conservative assumptions in the modelling of the PWHT.

Since measurement data was not available, sensitivity study data using Type 308 L weld material properties instead of Alloy 82 have been compared with measurements that were made in a similar test piece.

7. References

1. Abaqus/CAE 6.10-3, Dassault Systèmes Simulia Corporation, Providence, RI.

8. Copyright

© 2014 Rolls-Royce plc

The information in this document is the property of Rolls-Royce plc and may not be copied or communicated to a third party, or used for any purpose other than that for which it is supplied without the express written consent of Rolls-Royce plc.

Rolls-Royce plc has provided consent to Dassault Systèmes Simulia Corporation to publish this Paper with appropriate credit given to the author(s) and his/her/their employer. Therefore, Dassault Systèmes Simulia Corporation hereby granted the right and license to publish the Paper in printed, electronic other medium for the 2014 SIMULIA Community Conference, and as a separate work. This is not intended to transfer any copyright in the paper.